Appendix F: Waist Radius Measurement of Gaussian Beams

Abstract: OI-RD microscopes scan focused Gaussian laser beams across a microarray to provide spatial maps of the reflectivity difference. I review some properties of Gaussian beams, with particular emphasis on the waist diameter, which governs the best resolution achievable with an OI-RD microscope. Data is presented demonstrating a scanning knife-edge method for measuring a Gaussian beam waist; this method was used to measure the waist diameter for several OI-RD microscopes.

F.1 Introduction

The output beams of lasers do not exhibit a uniform cross sectional irradiance profile. Typically, the irradiance follows a Gaussian ($\exp\left(-r^2\right)$) profile with distance from the beam axis. Such beams are called *Gaussian beams* or *TEM_{00} beams*[1]. For many phenomena (for example, reflection and transmission at planar interfaces), the behavior of the Gaussian output beam of a laser is well described using geometric optics or a plane wave model. However, the long-wavelength geometric optics approximation fails near a focal point of the beam and the theory of diffraction must be employed to explain the beam properties there. In practical terms, even with perfectly aberration free lenses, a Gaussian beam cannot be focused to a geometric point. For scanning OI-RD microscopes using focused Gaussian laser beams, it is important to know the size of the diffraction-limited (smallest achievable) spot since this determines the highest lateral resolution achievable with the microscope. In this appendix, Gaussian beams and their descriptive parameters (waist radius, divergence angle, Rayleigh range, confocal length, and M^2 parameter) are reviewed. Then an experimental method is presented for measuring these parameters by "slicing" the beam with a knife-edge.

F.2 Gaussian Beam Parameters

Explicit derivations of the properties of Gaussian beams, from either direct solution of the paraxial wave equation or by evaluating the Kirchoff-Fresnel diffraction integral (in the paraxial approximation), can be found in most textbooks on laser physics [1-3]. The results are summarized here. Assume that the

[1] Similar notation is used for Hermite-Gaussian and Laguerre-Gaussian beam modes, so in general one must specify which basis set is being used. However, the 00 mode is equivalent for both basis sets. Lasers tend to resonate in Hermite-Gaussian modes due to slight astigmatism from Brewster windows in the resonant cavity.

beam under consideration is propagating along the z-axis in vacuum and that the value of the electric field in the xy-plane has a Gaussian profile

$$\tilde{\mathbf{E}}\left(x,y,z=0,t\right)=\tilde{\mathbf{E}}_0\exp\left[\frac{-\left(x^2+y^2\right)}{w_0^2}\right]\exp\left(-i\omega t\right), \tag{F.1}$$

where ω is the angular frequency of the beam, w_0 is a constant (called the *waist radius*), and $\tilde{\mathbf{E}}_0$ is a constant complex vector (thus, it is assumed that the polarization is uniform throughout the xy-plane). The corresponding irradiance ($I=\tilde{\mathbf{E}}\cdot\tilde{\mathbf{E}}^*$) profile in the xy-plane is

$$I\left(x,y,z=0,t\right)=I_0\exp\left[\frac{-2\left(x^2+y^2\right)}{w_0^2}\right]. \tag{F.2}$$

Eq. (F.2) shows that the waist radius can be interpreted as the distance from the beam axis at which the irradiance has fallen to $1/e^2=13.5\%$ of its maximum value. Using Eq. (F.1) as a boundary condition, one can shown that (within the paraxial approximation) the electric field everywhere else in space is given by

$$\tilde{\mathbf{E}}\left(x,y,z,t\right)=\tilde{\mathbf{E}}_0\frac{w_0}{w\left(z\right)}\exp\left[\frac{-\left(x^2+y^2\right)}{\left(w\left(z\right)\right)^2}\right]\exp\left[i\frac{k\left(x^2+y^2\right)}{2R\left(z\right)}\right]\exp\left[ikz-i\omega t+i\phi\left(z\right)\right], \tag{F.3}$$

where λ is the vacuum wavelength of the beam,

$$k=\omega/c=2\pi/\lambda\,, \tag{F.4}$$

$$w\left(z\right)=w_0\sqrt{1+\left(\frac{\lambda z}{\pi w_0^2}\right)^2}\,, \tag{F.5}$$

$$R\left(z\right)=z\left[1+\left(\frac{\pi w_0^2}{\lambda z}\right)^2\right], \tag{F.6}$$

and

$$\phi\left(z\right)=\tan^{-1}\left(\frac{\lambda z}{\pi w_0^2}\right). \tag{F.7}$$

The corresponding irradiance profile is

$$I\left(x,y,z,t\right)=I_0\left(\frac{w_0}{w\left(z\right)}\right)^2\exp\left[\frac{-2\left(x^2+y^2\right)}{\left(w\left(z\right)\right)^2}\right]. \tag{F.8}$$

Therefore, the irradiance profile in any plane parallel to the xy-plane (i.e. perpendicular to the direction of propagation) is also Gaussian. The *beam radius* in any such plane is defined as the radius at which the irradiance has fallen to $1/e^2$ of its maximum value at the center of the beam. Thus, $w\left(z\right)$ describes the z dependence of the beam radius. The *beam waist* is the position where the beam radius is minimized. It is clear from Eq. (F.5) that this occurs at $z=0$ and, therefore, the waist radius w_0 is the smallest beam radius

in the beam. The function $R(z)$ describes the radius of curvature of the spherical beam wavefronts (the wavefront is planar at the beam waist) and $\phi(z)$ is a phase factor that changes continuously by 180º in a region near the beam waist. The geometric properties of Gaussian beams are illustrated in Figure F.1.

The irradiance profile of a Gaussian beam is completely determined by the vacuum wavelength λ, waist radius w_0, maximum irradiance I_0, propagation direction, and beam waist location. However, there are several other useful parameters used to describe various properties of the Gaussian beam. The *beam divergence angle* θ describes the spreading of the Gaussian beam from the beam waist. It is the angle between the $1/e^2$ irradiance contour and the beam axis far from the beam waist (where $w(z)$ is approximately linear) and is given by

$$\theta \equiv \frac{\lambda}{\pi w_0}. \tag{F.9}$$

Thus, the smaller the beam waist, the faster the beam will diverge (this type of behavior is characteristic of diffraction). In the region near the beam waist, the beam radius is nearly constant. The length of this region is a measure of the degree of collimation of the Gaussian beam. The *Rayleigh range* z_R is defined to be the distance along the beam (from the beam waist) at which the cross sectional area of the $1/e^2$ irradiance contour is twice the area of the contour at the beam waist. The Rayleigh range is given by

$$z_R \equiv \frac{\pi w_0^2}{\lambda}. \tag{F.10}$$

The region of the beam where $|z| \le z_R$ is called the *confocal region* of the beam and the length $2z_R$ is called the *confocal length*. The smaller the beam waist, the smaller the Rayleigh range; thus, to have a highly collimated Gaussian beam over a long distance, the beam waist must be large. It is convenient to rewrite Eqs. (F.5)–(F.7) in terms of the Rayleigh range

$$w(z) = w_0\sqrt{1+\left(\frac{z}{z_R}\right)^2}, \tag{F.11}$$

$$R(z) = z\left[1+\left(\frac{z_R}{z}\right)^2\right], \tag{F.12}$$

and

$$\phi(z) = \tan^{-1}\left(\frac{z}{z_R}\right). \tag{F.13}$$

Eqs. (F.9) and (F.10) describe an ideal TEM_{00} beam mode. In practice, real Gaussian laser beams are predominantly TEM_{00}, but also have contributions from higher order modes (due to aberrations from windows, lenses, and mirrors in the optical system, for example). Furthermore, near a very sharp focus, the

paraxial approximation (used in the derivation of Eq. (F.3)) fails. Such effects cause the divergence angle and Rayleigh range of real Gaussian beams to differ from their ideal values. Empirically, these deviations are often well accounted for by introducing an "*M-squared" parameter* (M^2) such that the beam divergence and Rayleigh range are given by

$$\theta \equiv \frac{M^2 \lambda}{\pi w_0} \tag{F.14}$$

and

$$z_R \equiv \frac{\pi w_0^2}{M^2 \lambda}. \tag{F.15}$$

With these modified definitions, Eqs. (F.3), (F.8), and (F.11)–(F.13) continue to hold.

F.3 Gaussian Beams In Optical Systems

A common task in optical experiments is to take a given Gaussian beam (typically the output of a laser) and to modify the beam properties using appropriate optics (lenses, prisms, mirrors, etc.). Geometrical optics can be generalized to encompass Gaussian beams. In particular, the central beam axis of a Gaussian beam can be traced using standard methods (thin lens ray traces, paraxial ray traces, or exact Snell's law ray traces, as appropriate). Within the paraxial approximation, ray propagation through an optical system can be described using ray transfer matrices (often called *ABCD* matrices) [1-3]. In addition to tracing the Gaussian beam path, the effect an optical component has upon the radius of curvature and beam radius can be determined using the *ABCD* matrix of the component. The *complex radius of curvature* $\tilde{q}$ of a Gaussian beam is defined by

$$\frac{1}{\tilde{q}} \equiv \frac{1}{R} + i\frac{\lambda}{\pi w^2}. \tag{F.16}$$

If $\tilde{q}$ is incident upon the component and $\tilde{q}'$ emerges from the component, then it can be shown [1-3] that

$$\tilde{q}' = \frac{A\tilde{q} + B}{C\tilde{q} + D}. \tag{F.17}$$

Figure F.2 illustrates the important situation of focusing a Gaussian beam using a thin converging lens (such as might be found in a scanning OI-RD microscope). Using the *ABCD* matrix for the thin positive lens [1-3] and Eq. (F.17), the relationships between the input and output beams are

$$\frac{1}{w_{02}^2} = \frac{1}{w_{01}^2}\left(1 - \frac{z_1}{f}\right)^2 + \frac{1}{\left(f\theta_1\right)^2} \tag{F.18}$$

and

$$z_2 = f + \frac{f^2\left(z_1 - f\right)}{\left(z_1 - f\right)^2 + z_{R1}^2}. \tag{F.19}$$

If the input waist is much larger than the output waist ($w_{01} \gg w_{02}$) and the confocal region of the input is near the front focal point of the lens ($z_{R1} \gg z_1 - f$), then the approximate output beam waist radius and position are

$$w_{02} \cong f\theta_1 \tag{F.20}$$

and

$$z_2 \cong f\ . \tag{F.21}$$

In this limit, Eq. (F.20) shows that the focused beam waist decreases with smaller focal length and with higher input beam collimation (smaller input beam divergence angle), while Eq. (F.21) indicates that the waist is located at essentially the back focal point of the lens.

F.4 The Knife-Edge Test for Locating a Focus

The *knife-edge test*, illustrated in Figure F.3, is a simple method for approximately locating the position of a focus (or Gaussian beam waist) when it is located in air. A knife-edge is mounted on a translation stage and moved across the beam while looking at the transmitted light on a screen. From simple geometric optics, if the knife-edge is before the focus, the shadow on the screen will be on the *opposite* side and will move in the opposite direction of the knife-edge. Similarly, if the knife-edge is behind the focus, the shadow on the screen will be on the *same* side and will move in the same direction as the knife-edge. At the focus, the transmitted beam will tend to blink on and off, with no discernable shadow motion (dependent, of course, on the waist radius and translation resolution).

F.5 Scanning Knife-Edge Method for Measuring a Waist Radius

Figure F.4 illustrates the *scanning knife-edge* method for measuring the waist radius of a focused Gaussian beam. In this method, a knife-edge (for example, a razor blade) is mounted on a motorized translation stage and scanned across the beam. The unobstructed portion of the beam is relayed to a photodetector and its intensity is recorded as the knife-edge "slices" the Gaussian beam. From this profile, the beam radius at the particular *z* coordinate of the knife-edge can be determined. The beam is modulated using a rotary optical chopper in order to make the intensity measurement less susceptible to ambient light and to improve the signal-to-noise ratio for obstructed beams. The photodetector signal is Fourier analyzed (with

a lock-in amplifier, a digital spectral power analyzer, or a computer-based spectral power analyzer) to determine the transmitted power at the chopper frequency.

To measure the waist radius, one can either: (A) approximately locate the waist position using the knife-edge test and then measure the beam radius at that location or, (B) measure the beam radius as a function of z (by mounting the razor on a second translation stage) in the vicinity of the beam waist. Method (B) gives the most accurate measurement of the waist radius. It also accurately locates the waist position and allows the M^2 parameter of the beam to be determined. An analysis of Method (B) is detailed in this section.

The most convenient coordinates to use in such an experiment are the arbitrarily located positions of the razor blade translation stages. Assume that the beam propagates in a direction parallel to the z-axis and that its waist is located at the (initially unknown) coordinates (x_0, y_0, z_0). Also, assume that the knife-edge is parallel to the y-axis so that the x-axis is the "slicing" direction. The beam power $P(x,z)$ detected by the photodiode as a function of the knife-edge's transverse position x and axial position z is obtained by integrating the Gaussian beam irradiance profile over all y and the unobstructed range of x. The result is

$$\begin{aligned} P(x,z) &= p(z)\int_x^{\infty} \exp\left[\frac{-2(x-x_0)^2}{(w(z))^2}\right] dx \\ &= \frac{P_0}{2}\operatorname{erfc}\left[\frac{\sqrt{2}(x-x_0)}{w(z)}\right], \end{aligned} \tag{F.22}$$

where $\operatorname{erfc}(x)$ is the complementary error function [4],

$$p(z) = \sqrt{\frac{\pi}{2}} I_0 \frac{w_0^2}{w(z)}, \tag{F.23}$$

$$P_0 = \frac{\pi}{2} I_0 w_0^2, \tag{F.24}$$

and

$$\begin{aligned} w(z) &= w_0\sqrt{1+\left(\frac{M^2\lambda(z-z_0)}{\pi w_0^2}\right)^2} \\ &= w_0\sqrt{1+\left(\theta\frac{(z-z_0)}{w_0}\right)^2}. \end{aligned} \tag{F.25}$$

$P(x,z)$ is a sigmoidal function that falls from a maximum value of P_0 (for a completely unobstructed beam, $x \ll x_0$), to $P_0/2$ at $x = x_0$ (half obstructed beam), to zero (for a completely obstructed beam, $x \gg x_0$) over the approximate interval $[x_0 - 2w(z), x_0 + 2w(z)]$. This interval must be sampled particularly densely to extract an accurate value for $w(z)$ from an experimentally measured $P(x,z)$ vs. x curve.

Furthermore, this analysis assumes that the slice is made perpendicular to the beam; care must be taken to ensure that the knife-edge translation is indeed perpendicular to the beam. There are three methods for determining $w(z)$:

Method (1): Experimental $P(x,z)$ vs. x data can be directly fitted to Eq. (F.22) using nonlinear fitting software with P_0, x_0, and $w(z)$ as fit parameters. Data points in the tails should not be given undue weight. One way to achieve this is to sample the tails more sparsely and to not include points outside the interval $\left[x_0 - 4w(z), x_0 + 4w(z)\right]$.

Method (2): Eq. (F.22) can be recast as a quadratic equation, which can then be fit in the wide range of software and calculators capable of performing polynomial regression. First, the experimentally sampled $P(x,z)$ vs. x curve must be numerically differentiated, giving

$$\frac{\partial P}{\partial x} = -p(z)\exp\left[\frac{-2(x-x_0)^2}{(w(z))^2}\right]. \tag{F.26}$$

Numerical differentiation is particularly susceptible to noise in the data, especially in the tails where the nominal value of the derivative is nearly zero. If a simple difference quotient algorithm is used to numerically differentiate the data, it may be helpful to smooth the data before differentiating and to exclude points outside the interval $\left[x_0 - 3w(z), x_0 + 3w(z)\right]$ from the fit. A sufficiently narrow smoothing window should be applied to avoid artificially broadening the apparent value of $w(z)$. Median filters are particularly robust for this purpose because they eliminate punctate noise with minimal blurring. Finally, by taking the logarithm of Eq. (F.26), the following quadratic equation is obtained:

$$\ln\left|\frac{\partial P}{\partial x}\right| = \left[\frac{-2}{(w(z))^2}\right]x^2 + \left[\frac{4x_0}{(w(z))^2}\right]x + \left[\ln p(z) - \frac{2x_0^2}{(w(z))^2}\right]. \tag{F.27}$$

Thus, the parameters $p(z)$, x_0, and $w(z)$ can be determined from the coefficients of a quadratic fit to the experimental $\ln\left|\partial P/\partial x\right|$ vs x data.

Method (3): The distance between the knife-edge positions where 90% and 10% of the maximum power is transmitted can be used to determine $w(z)$. Using Eq. (F.22) this distance is found to be

$$w(z) \cong 0.780\cdot\left(x_{10\%} - x_{90\%}\right) \tag{F.28}$$

where $P(x_{10\%}, z) = 0.10\cdot P_0$ and $P(x_{90\%}, z) = 0.90\cdot P_0$.

To obtain accurate and independent values of w_0 and M^2, experimental $w(z)$ vs. z data must be fit to Eq. (F.25). The confocal region must be sampled particularly densely to obtain an accurate value for w_0. However, it is also important to include several points well outside the confocal region in order to get an accurate independent value of M^2. Eq. (F.25) is easily fit by recasting it as a quadratic equation

$$\left(w(z)\right)^2 = \left[\theta^2\right]z + \left[-2\theta^2 z_0\right]z + \left[w_0^2 + \theta^2 z_0^2\right]. \tag{F.29}$$

Thus, the parameters w_0, θ, and z_0 can be determined from the coefficients of a quadratic fit to the experimental $\left(w(z)\right)^2$ vs z data. M^2 can be determined using w_0 and θ. This analysis assumes that the slicing plane is translated parallel to the beam axis; care must be taken to ensure that this is so.

Figure F.5 contains experimental data illustrating the methods discussed in this section. For this experiment, a Lasos Lasertechnik He-Ne laser (model LGK 7828-1) was focused with a 10× infinity corrected long-working distance objective (Mitutoyo 10× M Plan Apo). The laser parameters were: wavelength $\lambda = 632$ nm, power 5 mW, divergence angle $\theta = 0.1$ rad, and a nominal TEM_{00} transverse mode. The beam diameter at the back aperture of the objective was ~ 3 mm. Figure F.5(A) shows a representative scanning knife-edge transmitted power profile of the beam away from the waist. The circles are the normalized experimental data points and the solid curve is a fit of Eq. (F.22) to the data. The nonlinear fit gives a beam radius of 92.7 ± 0.3 μm, where the uncertainty is the estimated standard deviation determined by the non-linear fit algorithm (Igor Pro 6.01, Wavemetrics). In comparison, the radius determined from Eq. (F.28) is 90.9 μm, in fair agreement with the nonlinear fit. The discrepancy between the two methods is most likely due to deviation of the profile from a true TEM_{00} mode. In particular, small but systematic differences in the fit and data are seen just before the $x_{90\%}$ point and after the $x_{10\%}$ point. Figure F.5 (B) and Figure F.5 (C) show the radius profile of the focused laser beam obtained from a series of measurements such as the one shown in Figure F.5(A). The circles are the normalized experimental data points and the solid curve is a fit of Eq. (F.25) to the data. The nonlinear fit gives a waist radius of $w_0 = 3.5 \pm 0.4$ μm and Raleigh range $z_R = 58 \pm 7$ μm, where the uncertainty is the estimated standard deviation determined by the non-linear fit algorithm. Furthermore, slight deviation of the profile from a TEM_{00} mode is indicated by the measured M^2 value of 1.06.

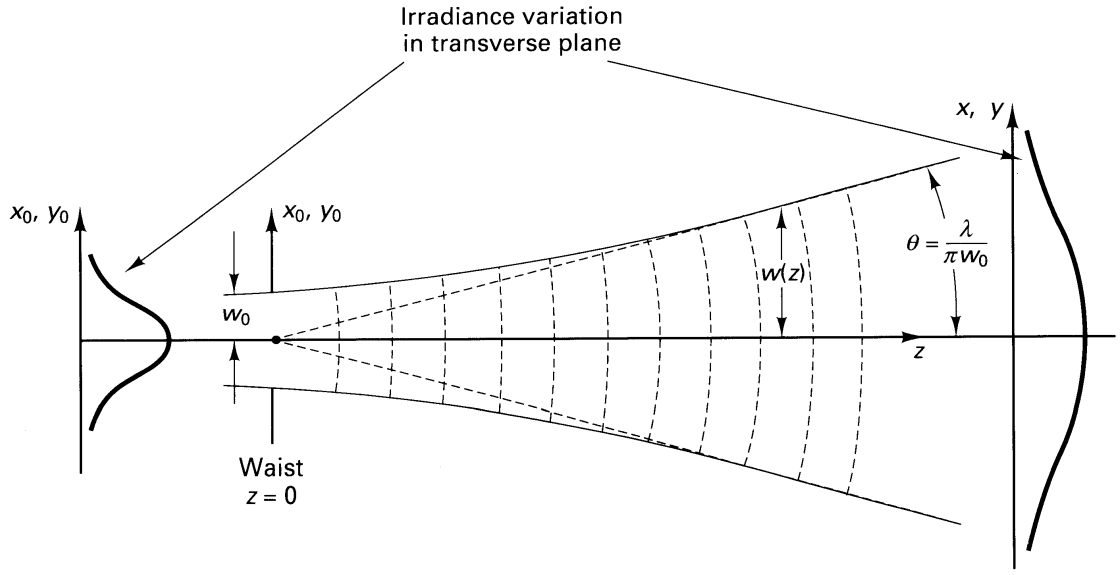

Figure F.1 Gaussian Beam Parameters

Figure reproduced from Reference [1].

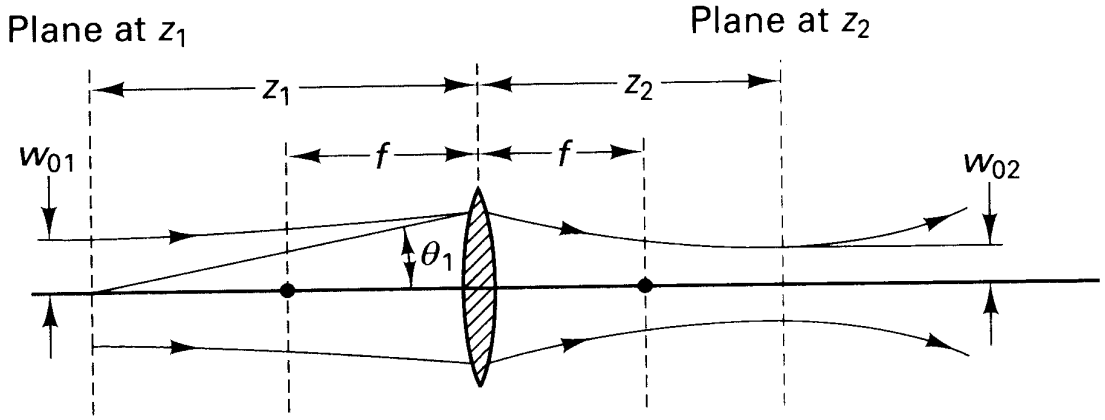

Figure F.2 Focusing A Gaussian Beam

Figure reproduced from Reference [1].

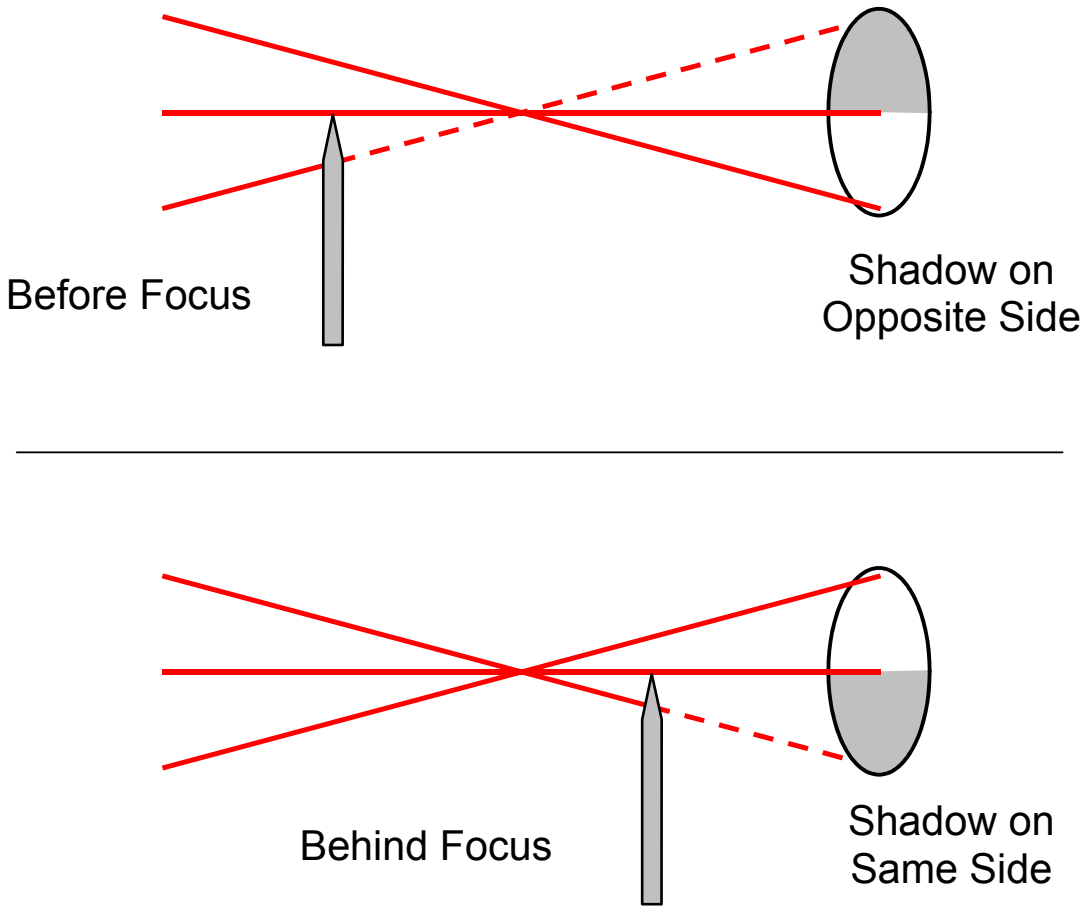

Figure F.3 The Knife-Edge Test For Locating A Focus

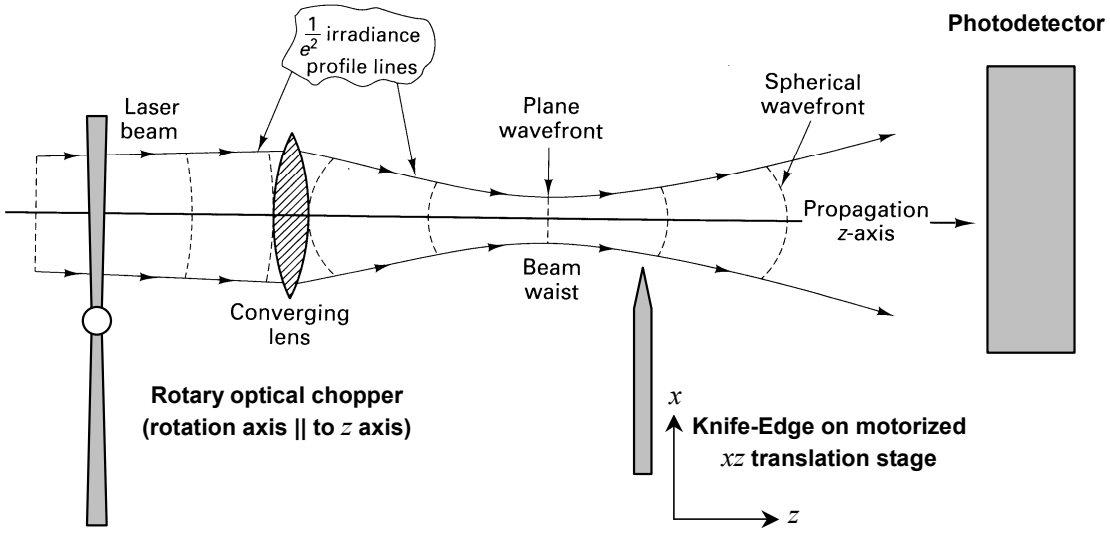

Figure F.4 The Scanning Knife-Edge Method For Measuring A Waist Radius

Figure reproduced and modified from Reference [1].

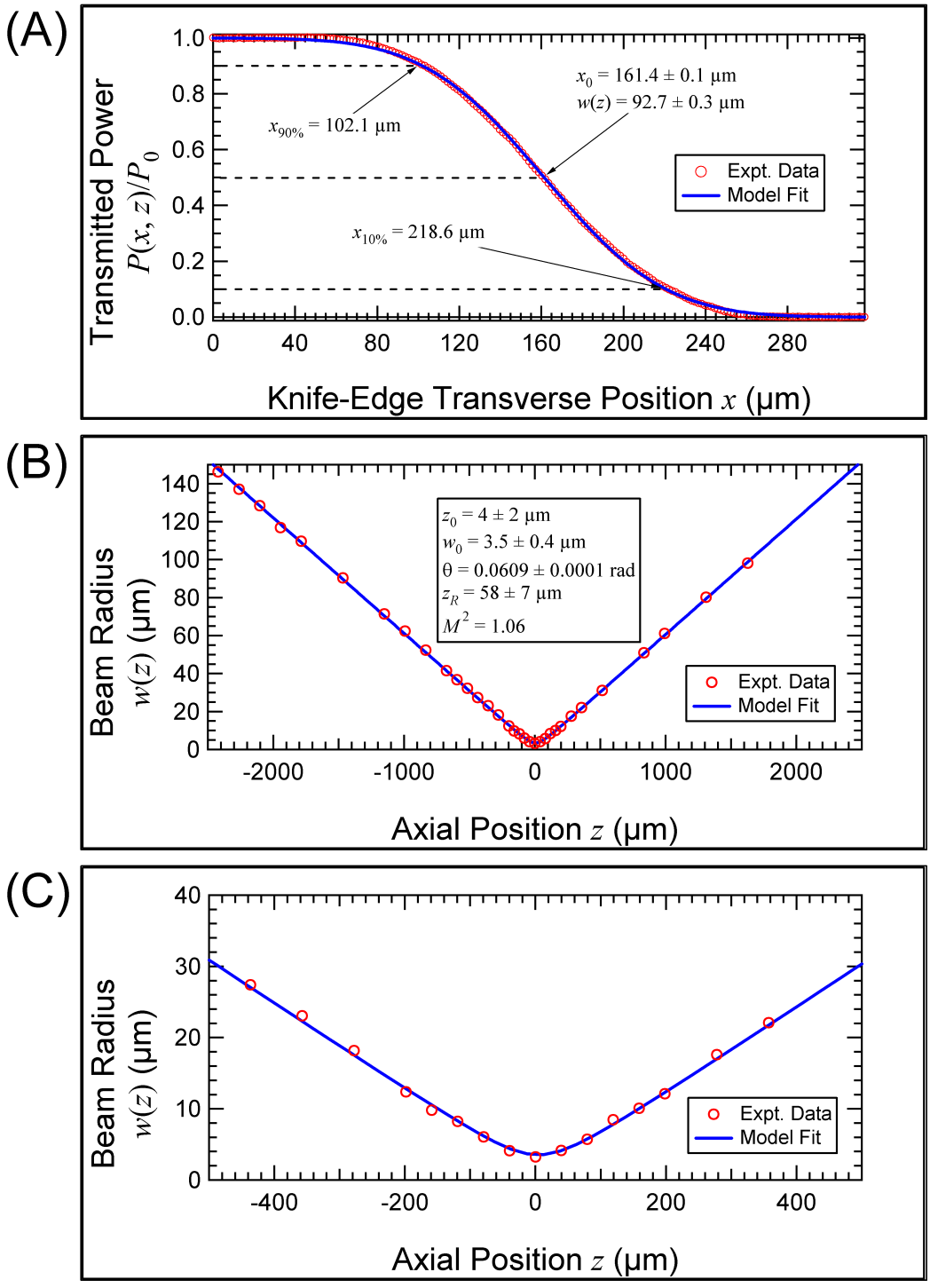

Figure F.5 Sample Experimental Scanning Knife-Edge Data

(A) Representative experimental transmitted power profile of a He-Ne laser beam. (B) Experimental radius profile of a focused He-Ne laser beam. (C) Same profile as (B), but zoomed in near the beam waist.

References

1. Pedrotti, F.L. and L.S. Pedrotti, Introduction to optics., 2nd ed. (Pearson Prentice Hall, 1993).

2. Siegman, A.E., Lasers (University Science Books, 1986).

3. Yariv, A., Quantum electronics, 3rd ed. (John Wiley & Sons, 1989).

4. Jeffrey, A., Handbook of mathematical formulas and integrals, 2nd ed. (Academic Press, 2000).